Remote Sens. **2015**, *7*, 14179-14199; doi:10.3390/rs71014179

OPEN ACCESS

remote sensing

ISSN 2072-4292

www.mdpi.com/journal/remotesensing

Article

Quantitative Estimation of Fluorescence Parameters for Crop Leaves with Bayesian Inversion

Feng Zhao [1,*], Yiqing Guo [1], Yanbo Huang [2], Wout Verhoef [3], Christiaan van der Tol [3], Bo Dai [1], Liangyun Liu [4], Huijie Zhao [1] and Guang Liu [4]

1 School of Instrumentation Science and Opto-electronics Engineering, Beihang University, Beijing 100191, China; E-Mails: yguo_buaa@163.com (Y.G.); daibo_2007@163.com (B.D.); hjzhao@buaa.edu.cn (H.Z.)

2 United States Department of Agriculture-Agricultural Research Service, Crop Production Systems Research Unit, 141 Experiment Station Road, Stoneville, MS 38776, USA; E-Mail: Yanbo.Huang@ars.usda.gov

3 Faculty of Geo-Information Science and Earth Observation (ITC), University of Twente, P.O. Box 217, Enschede 7500 AE, The Netherlands; E-Mails: w.verhoef@utwente.nl (W.V.); c.vandertol@utwente.nl (C.T.)

4 Institute of Remote Sensing and Digital Earth, Chinese Academy of Sciences, No.9 Dengzhuang South Road, Haidian District, Beijing 100094, China; E-Mails: liuly@radi.ac.cn (L.L.); liuguang@radi.ac.cn (G.L.)

***** Author to whom correspondence should be addressed; E-Mail: zhaofeng@buaa.edu.cn; Tel./Fax: +86-10-8231-5884.

Academic Editors: Tao Cheng, Clement Atzberger and Prasad S. Thenkabail

Received: 31 March 2015 / Accepted: 22 October 2015 / Published: 27 October 2015

Abstract: In this study, backward and forward fluorescence radiance within the emission spectrum of 640–850 nm were measured for leaves of soybean, cotton, peanut and wheat using a hyperspectral spectroradiometer coupled with an integration sphere. Fluorescence parameters of crop leaves were retrieved from the leaf hyperspectral measurements by inverting the FluorMODleaf model, a leaf-level fluorescence model able to simulate chlorophyll fluorescence spectra for both sides of leaves. This model is based on the widely used and validated PROSPECT (leaf optical properties) model. Firstly, a sensitivity analysis of the FluorMODleaf model was performed to identify and quantify influential parameters to assist the strategy for the inversion. Implementation of the Extended Fourier Amplitude Sensitivity Test (EFAST) method showed that the leaf chlorophyll content and the

fluorescence lifetimes of photosystem I (PSI) and photosystem II (PSII) were the most sensitive parameters among all eight inputs of the FluorMODleaf model. Based on results of sensitivity analysis, the FluorMODleaf model was inverted using the leaf fluorescence spectra measured from both sides of crop leaves. In order to achieve stable inversion results, the Bayesian inference theory was applied. The relative absorption cross section of PSI and PSII and the fluorescence lifetimes of PSI and PSII of the FluorMODleaf model were retrieved with the Bayesian inversion approach. Results showed that the coefficient of determination (R^2) and root mean square error (RMSE) between the fluorescence signal reconstructed from the inverted fluorescence parameters and measured in the experiment were 0.96 and 3.14 $\times 10^{-6}$ W m^{-2} sr^{-1} nm^{-1}, respectively, for backward fluorescence, and 0.92 and 3.84 $\times 10^{-6}$ W m^{-2} sr^{-1} nm^{-1} for forward fluorescence. Based on results, the inverted values of the fluorescence parameters were analyzed, and the potential of this method was investigated.

Keywords: chlorophyll fluorescence; FluorMODleaf; model inversion; Bayesian approach; hyperspectral remote sensing; radiative transfer

1. Introduction

Chlorophyll fluorescence (ChlF) is considered a promising tool to effectively assess photosynthetic rates of green plants [1] and to monitor stress conditions of crops [2,3]. As a result, quantitative analysis of the ChlF signal using remote sensing techniques has been conducted extensively in recent years [1,4], along with development of leaf ChlF radiative transfer models that have improved understanding of the interactions of sunlight with plant leaves [5–7].

Leaf ChlF radiative transfer models can be used to simulate leaf backward (the emission direction opposite to the direction of the excitation light) and forward (the emission direction same as the direction of the excitation light) ChlF spectra as a function of the incident light, and the leaf biochemical and fluorescence parameters. The FluorMOD project began in 2002 with a goal of developing an integrated leaf-canopy fluorescence model [8]. As a subcomponent of the integrated model, FluorMODleaf [6,8] is a leaf-level fluorescence model based on the PROSPECT model [9,10] and can be used to calculate the radiative transfer of ChlF in plant leaves. Besides the FluorMODleaf model, other leaf ChlF models were also developed. For example, FLUSPECT [7] is another leaf ChlF radiative transfer model that is also based on the PROSPECT model and uses fluorescence quantum efficiencies of photosystem I (PSI) and photosystem II (PSII) as inputs. Computer-based Monte Carlo methods were also developed to simulate the leaf-level ChlF signal [5].

The FluorMODleaf model has a total of eight input parameters [6]. Besides five original parameters of the PROSPECT-5 model [9], *i.e.*, leaf structure parameter N, chlorophyll content C_{ab}, carotenoid content C_{ar}, water content C_w, and dry matter content C_m, three fluorescence parameters were newly introduced, *i.e.*, the relative absorption cross section of PSI and PSII, δ, and fluorescence lifetimes of PSI and PSII, τ_I and τ_{II}. Definitions, units, and descriptions of the eight input parameters of the FluorMODleaf model are illustrated in Table 1. Outputs of FluorMODleaf model are the forward and

backward apparent spectral fluorescence yield (ASFY), besides leaf reflectance and transmittance. The FluorMODleaf model was evaluated using experimental datasets, and good agreement between the model-simulated and experimental data was shown [6]. However, the study on inversion of FluorMODleaf was not reported.

Table 1. The definitions, units, and descriptions of the eight input parameters of the FluorMODleaf model [6].

Parameter	Definition	Unit	Description
N	Leaf structure parameter	-	Number of compact layers specifying the average number of air/cell wall interfaces within the mesophyll.
C_{ab}	Chlorophyll a+b content	$\mu g \cdot cm^{-2}$	Mass of chlorophyll a+b per leaf area.
C_{ar}	Total carotenoid content	$\mu g \cdot cm^{-2}$	Mass of total carotenoid per leaf area.
C_w	Water content	$g\ cm^{-2}$	Mass of water per leaf area.
C_m	Dry matter content	$g\ cm^{-2}$	Mass of dry matter per leaf area.
δ	Relative absorption cross section ratio	-	The relative distribution of light between the two photosystems, which can be approximated by the product of the PSII/PSI antenna size ratio.
τ_I	Fluorescence lifetimes of photosystem I (PSI)	ns	Average time the chlorophyll molecule stays in its excited state before emitting a photon from isolated PSI complexes.
τ_{II}	Fluorescence lifetimes of photosystem II (PSII)	ns	Average time the chlorophyll molecule stays in its excited state before emitting a photon from isolated PSII complexes.

The relative absorption cross section of PSI and PSII (δ) and fluorescence lifetimes of PSI and PSII (τ_I and τ_{II}) are critical foliar parameters defining the fluorescence emission properties of plant leaves. However, these fluorescence parameters (1) are difficult to measure directly; (2) are species-dependent; and (3) vary greatly under different environmental conditions [6]. Therefore, quantitative retrieval of these fluorescence parameters from leaf hyperspectral fluorescence data by inverting a physically-based ChlF radiative transfer model would be a non-destructive and effective method to retrieve these parameters.

Compared with the reflected and transmitted signals of leaves, leaf ChlF is very weak. Therefore, in order to achieve stable inversion results, additional information and inversion strategy should be used to improve the accuracy of the inverted parameters. Bayesian inversion approach is a suitable alternative to impose *a priori* information on the inversion process and has shown potential for the inversion of remote sensing models [11]. By injecting reliable *a priori* information into the inversion process, a more stable solution for the unknown parameters can be achieved. As an effective way to alleviate ill-posed problems in the inversion process, the Bayesian inversion approach has been used in studies for the retrieval of terrestrial parameters from remote sensing data [12–14].

The objectives of this study were (1) to perform a sensitivity analysis of the FluorMODleaf model in order to identify and quantify influential parameters; (2) to retrieve the parameters of FluorMODleaf model using the experimental datasets. Firstly, a sensitivity analysis of the FluorMODleaf model was performed using the Extended Fourier Amplitude Sensitivity Test (EFAST) method. Based on sensitivity analysis results, the FluorMODleaf model was inverted using the experimental datasets acquired for four types of crop leaves. In order to achieve stable inversion results, Bayesian theory was introduced into the inversion process. The relative absorption cross section of PSI and PSII (δ) and fluorescence lifetimes

of PSI and PSII (τ_I and τ_{II}) were then estimated with the Bayesian inversion approach of the FluorMODleaf model. Finally, the inversion results were validated and analyzed.

2. Materials and Methods

2.1. Experimental Datasets

Datasets at leaf level for four crop leaves were used in this study, and two field experiments were conducted. For each leaf, hyperspectral data and the biochemical content were obtained. Two leaves (for wheat) or three (for soybean, cotton and peanut) with similar color, height in the plant and physiological condition by visual inspection were chosen as a group for measurement of reflectance, transmittance, backward and forward fluorescence, and biochemical content. Then, data averages from these two or three leaves were used as a group for subsequent inversion.

The first experiment was conducted for winter wheat (*Triticum*) at the Beijing Academy of Agriculture and Forestry Sciences (39.942 °N, 116.277 °E) on 8 May 2014. Eight green leaves were measured with a hyperspectral spectroradiometer coupled with an integration sphere during 10:00–18:00 Beijing time.

The second experiment was conducted at the Huailai Remote Sensing Test Site (40.349 °N, 115.785 °E), Chinese Academy of Sciences, which is located at Huailai County, Hebei Province, China, during 15–19 September 2014. Three crops, soybean (*Glycine max*), cotton (*Gossypium*) and peanut (*Arachis hypogaea*), were targeted in the experiment. In the experiment, three leaves as a group were used for the experiment every hour from 9:00–18:00 for soybean, 9:00–15:00 for cotton, and 9:00–17:00 for peanut. Twenty-seven soybean leaves, 18 cotton leaves and 24 peanut leaves were measured in the experiment. Leaves from different heights and physiological conditions were measured in order to make the datasets more representative. Among them, a group of three senescent leaves with brown color for peanut was measured to compare with green leaves.

Similar to the measurement protocol of Zarco-Tejada *et al.* [15] and Zhang [16], the leaf hyperspectral data were measured using a LI-COR 1800-12 system integrating sphere apparatus (LI-COR Inc., Lincoln, NE, USA) coupled with an ASD FieldSpec Pro spectroradiometer (ASD Inc., Boulder, CO, USA) and removable filter, as shown in Figure 1. However, different from the protocol of using a long-pass filter by Zarco-Tejada *et al.* [15], a short-pass filter was used instead in front of the lamp in our experiment with irradiance longer than 640 nm being cut-off. Therefore, the reflected/transmitted signal should be filtered out in wavelengths longer than 640 nm, and the signal measured by the spectroradiometer within the wavelength range of 640–850 nm would be composed mainly of the emitted ChlF signal. The spectral data were measured *in situ* with leaves attaching to their stems. The hyperspectral measurements were conducted under guidance of the LI-COR integrating sphere manual [17]. The spectral resolution and spectral sampling interval of the spectroradiometer are 3 nm and 1 nm, respectively. An integration time of 1.09 s was used for all the measurements.

It is worth noting that the radiance of the lamp in the experiment was very low, compared with the solar radiance under natural conditions. Therefore, the fluorescence radiance measured in this experiment would be lower than that under natural conditions, because the magnitude of the fluorescence radiance is proportional to the magnitude of the excitation radiance [8]. A typical radiance distribution

of the lamp with the short-pass filter is shown in Figure 2. Lamp's radiance passing through the filter is close to zero in the fluorescence emission wavelengths (640–850 nm), except for the initial parts of the cut-off wavelengths because of the instrument limit.

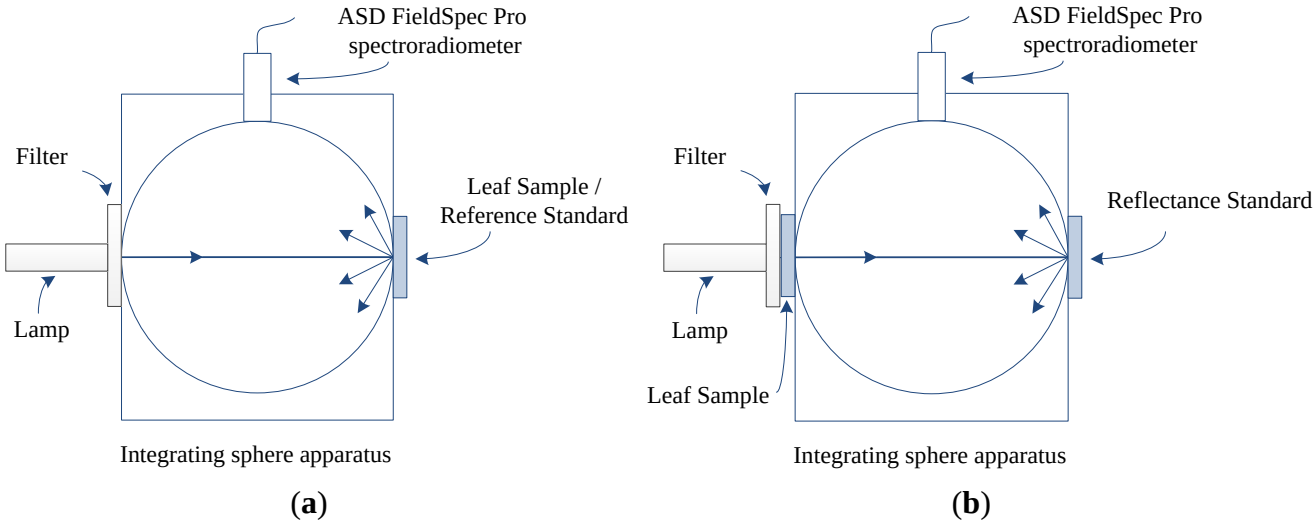

Figure 1. The experimental setup for leaf hyperspectral measurement. (**a**) Measurement configuration for leaf reflectance and backward fluorescence; (**b**) Measurement configuration for leaf transmittance and forward fluorescence.

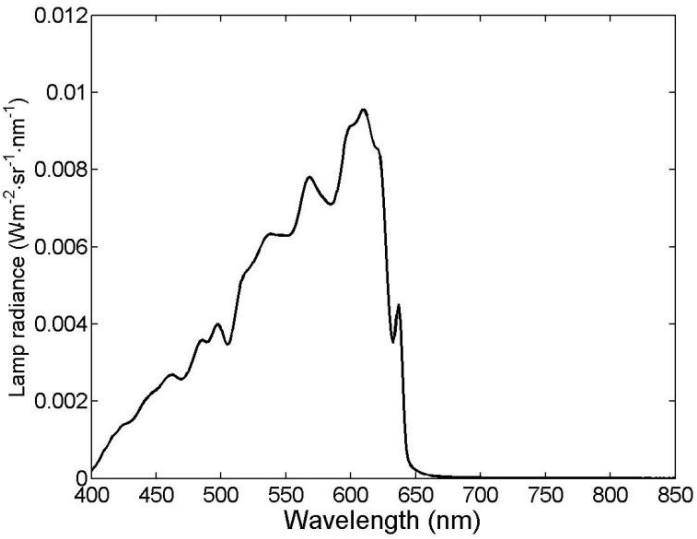

Figure 2. An example of radiance distribution of the lamp with the short-pass filter.

Three measurements of leaf reflectance and backward fluorescence were acquired by placing leaf sample as shown in Figure 1a: radiance of the leaf sample (Lb_{ls}^{on}), reference standard (Lb_{rs}^{on}), and dark current (Lb_{dc}^{on}). Then, another three measurements without the filter were acquired: radiance of the leaf sample (Lb_{ls}^{off}), reference standard (Lb_{rs}^{off}), and dark current (Lb_{dc}^{off}). The reflectance (R_{leaf}) and backward fluorescence radiance (F_b) of the leaf sample can be calculated as:

$$R_{leaf} = \frac{Lb_{ls}^{off} - Lb_{dc}^{off}}{Lb_{rs}^{off} - Lb_{dc}^{off}} \cdot R_{ref} \quad (1)$$

$$F_b = (Lb_{ls}{}^{on} - Lb_{dc}{}^{on}) - (Lb_{rs}{}^{on} - Lb_{dc}{}^{on}) \cdot R_{leaf} \quad (2)$$

where R_{ref} is the reflectance of the reference standard. The first part of the right side of the Equation (2) includes both mostly fluorescence emission by the leaf, and a small residual radiance reflected by the leaf, because transmittance of the filter is not exactly zero. The second part is added to correct the instrument limit.

To measure the transmittance and forward fluorescence, the leaf sample was moved to the front of the lamp, as shown in Figure 1b. Similarly, three measurements with the filter were acquired: radiance of the leaf sample ($Lf_{ls}{}^{on}$), reference standard ($Lf_{rs}{}^{on}$), and dark current ($Lf_{dc}{}^{on}$). Then, another three measurements without the filter were acquired: radiance of the leaf sample ($Lf_{ls}{}^{off}$), reference standard ($Lf_{rs}{}^{off}$), and dark current ($Lf_{dc}{}^{off}$). The transmittance (T_{leaf}) and forward fluorescence radiance (F_f) of the leaf sample can be calculated as:

$$T_{leaf} = \frac{Lf_{ls}{}^{off} - Lf_{dc}{}^{off}}{Lf_{rs}{}^{off} - Lf_{dc}{}^{off}} \cdot R_{ref} \quad (3)$$

$$F_f = (Lf_{ls}{}^{on} - Lf_{dc}{}^{on}) - (Lf_{rs}{}^{on} - Lf_{dc}{}^{on}) \cdot T_{leaf} \quad (4)$$

The output of the FluorMODleaf model is ASFY (in unit of nm^{-1}), which is defined as the ratio of the number of photons emitted by the leaf surface, per unit spectral bandwidth, to the number of incident photons [6,8], and not the fluorescence radiance measured in our experiment. Therefore, the output of the FluorMODleaf model was converted from ASFY into fluorescence radiance in order to be consistent with experimental data. The conversion was performed with the following formulae:

$$F_b(\lambda_{em}) = \int_{400}^{650} \frac{L_{lamp}{}^{on}(\lambda_{ex}) \cdot b_{\mathrm{mod}}(\lambda_{ex}, \lambda_{em}) \cdot \lambda_{ex}}{\lambda_{em}} d\lambda_{ex} \quad (5)$$

$$F_f(\lambda_{em}) = \int_{400}^{650} \frac{L_{lamp}{}^{on}(\lambda_{ex}) \cdot f_{\mathrm{mod}}(\lambda_{ex}, \lambda_{em}) \cdot \lambda_{ex}}{\lambda_{em}} d\lambda_{ex} \quad (6)$$

where λ_{ex} and λ_{em} represent the fluorescence excitation and emission wavelengths, respectively; b_{mod} and f_{mod} are the backward and forward ASFYs simulated by FluorMODleaf, respectively; $L_{lamp}{}^{on}$ is the radiance of the lamp with the filter used in the integrating sphere apparatus; F_b and F_f are the backward and forward fluorescence radiance calculated from the output of the FluorMODleaf model, which are now directly comparable with the quantities calculated respectively by Equations (2) and (4) in the experiment.

After the spectral measurements, the leaves were immediately cut from the plants, placed into black plastic bags surrounded by ice lumps, and taken to the laboratory for biochemical analysis. Chlorophyll a + b content (C_{ab}, in unit of $\mu g/cm^2$), total carotenoid content (C_{ar}, in unit of $\mu g/cm^2$), water content (C_w, in unit of g/cm^2), and dry matter content (C_m, in unit of g/cm^2) were measured for each leaf in the laboratory. Six leaf disks of 15 mm diameter were punched from each leaf sample, chopped into small pieces, and then dropped into the vial with ethanol solution and covered with aluminum foil. After 48 h in the dark environment, the solution was used for measuring the chlorophyll content and carotenoid content using a Shimadzu UV160U Spectrophotometer (Shimadzu Corp., Kyoto, Japan), using the method described by Lichtenthaler and Buschmann [18]. In order to measure the water and dry matter contents, the remaining portions of the leaves were scanned to determine leaf area and weighed to

measure their fresh weight. They were then oven-dried at 80 ℃ for 48 h, and reweighed to determine dry weight.

2.2. Sensitivity Analysis

Sensitivity analysis investigates the response of a model to variations of its input parameters by statistically calculating a limited, but representative number of simulations [19,20]. The analysis has been shown to be effective to help make strategy for the inversion of radiation transfer models [21]. Compared with the classic FAST (Fourier Amplitude Sensitivity Test) method for the sensitivity analysis of the models, which is only able to compute the first order sensitivity index, the Extended FAST (EFAST) method proposed by Saltelli *et al.* [20] allows the simultaneous computation of the first order and the total sensitivity indices for a given input parameter [21]. Therefore, in this study, the EFAST method was used for the sensitivity analysis of the FluorMODleaf model. The first order sensitivity index gives the independent effect of each parameter, while the total sensitivity index contains both independent effect of each parameter and the interaction effects with the others.

In the sensitivity analysis test, ranges of N, C_{ab}, C_{ar}, C_w, C_m, τ_I, τ_{II}, and δ were defined as 1–2.5, 0.4–76.8 μg/cm^2, 0–25.3 μg/cm^2, 0.0044–0.0340 g/cm^2, 0.0017–0.0331 g/cm^2, 0.034–0.1 ns, 0.3–2.0 ns, and 1.0–2.4, respectively, based on a previous study [6]. One thousand combinations of the parameters were randomly selected from their ranges as the inputs. Then, for each combination of the input parameters, the spectra of the backward and forward fluorescence were simulated by the FluorMODleaf model. All simulated fluorescence spectra combined with the corresponding selected values of input parameters were used as input data for the sensitivity analysis. Detailed procedure and formulae can be found in our previous studies [21,22].

2.3. Inversion Procedure

The inversion procedure includes two steps. In the first step leaf structural and biochemical parameters were inverted. Then, they were fixed at their inverted values for the second step to retrieve the rest three fluorescence parameters. In each step, an efficient global optimization algorithm based on simulated annealing, which was constructed and used in our former study [21], was applied in the inversion procedure to minimize the merit functions described below.

In the first step, the leaf structure parameter N was firstly inverted from the measured data of leaf reflectance (ρ_{leaf}) and transmittance (τ_{leaf}) by minimizing the following merit function $Fn(N)$, which is defined in the near-infrared wavelengths (λ) of 750–1300 where N is the most sensitive parameter among the input parameters of the PROSPECT-5 model [22]:

$$Fn(N) = \sum_{\lambda\in[750,1300]} \left\{ \left[\rho_{leaf}(\lambda) - \rho_{simu}(N, C_{ab}, C_{ar}, C_w, C_m, \lambda) \right]^2 + \left[\tau_{leaf}(\lambda) - \tau_{simu}(N, C_{ab}, C_{ar}, C_w, C_m, \lambda) \right]^2 \right\} \quad (7)$$

where ρ_{simu} and τ_{simu} are the leaf reflectance and transmittance simulated by the FluorMODleaf model. During this step, the biochemical parameters, *i.e.*, C_{ab}, C_{ar}, C_w, and C_m, were all maintained at their measured values.

Then, the other four parameters of the PROSPECT-5 model, including C_{ab}, C_{ar}, C_w, and C_m, were inverted by minimizing the following merit function $Fp(C_{ab},C_{ar},C_w,C_m)$, with the leaf structure parameter N being maintained at its inverted value obtained in the first step:

$$Fp(C_{ab},C_{ar},C_w,C_m) = \sum_{\lambda\in[400,2500]} \left\{ \left[\rho_{leaf}(\lambda) - \rho_{simu}(N,C_{ab},C_{ar},C_w,C_m,\lambda) \right]^2 + \left[\tau_{leaf}(\lambda) - \tau_{simu}(N,C_{ab},C_{ar},C_w,C_m,\lambda) \right]^2 \right\} \quad (8)$$

The merit function is defined on the spectral region of the PROSPECT-5 model (*i.e.*, 400–2500 nm).

In the second step of the inversion procedure, the fluorescence parameters τ_I, τ_{II}, and δ were retrieved from the measured leaf fluorescence spectra by minimizing the following merit function $Ff(\tau_I,\tau_{II},\delta)$, while the other parameters were all maintained at their inverted values obtained in the first step. The merit function $Ff(\tau_I,\tau_{II},\delta,N,C_{ab},C_{ar})$ was constructed with the Bayesian inversion theory [11,23]:

$$\begin{aligned} Ff(\tau_I,\tau_{II},\delta) = {} & \frac{1}{2}(F\boldsymbol{b}_{simu} - F\boldsymbol{b}_{meas})^{\mathrm{T}} \boldsymbol{C}_{nb}^{-1} (F\boldsymbol{b}_{simu} - F\boldsymbol{b}_{meas}) \\ & + \frac{1}{2}(F\boldsymbol{f}_{simu} - F\boldsymbol{f}_{meas})^{\mathrm{T}} \boldsymbol{C}_{nf}^{-1} (F\boldsymbol{f}_{simu} - F\boldsymbol{f}_{meas}) + \frac{1}{2}(\boldsymbol{x} - \boldsymbol{x}_{priori})^{\mathrm{T}} \boldsymbol{C}_x^{-1} (\boldsymbol{x} - \boldsymbol{x}_{priori}) \end{aligned} \quad (9)$$

where Fb_{meas} and Ff_{meas} are the backward and forward fluorescence measured in the experiment, respectively; $F\boldsymbol{b}_{simu}$ and $F\boldsymbol{f}_{simu}$ are the forward and backward fluorescence calculated by the output of FluorMODleaf model, as shown in Equations (5) and (6) respectively; $\boldsymbol{C}_{nb}$ and $\boldsymbol{C}_{nf}$ are the inaccuracy of model simulations and the noise covariance matrices for the measurements of the backward and forward fluorescence, respectively; $\boldsymbol{x}$ contains the unknown variables; $\boldsymbol{x}_{priori}$ is the *a priori* guess of the unknown variables; and $\boldsymbol{C}_x$ is the covariance matrix of the *a priori* variables. The expressions of these vectors and matrices are:

$$\begin{aligned} \boldsymbol{Fb}_{meas} &= [Fb_{meas}(\lambda_1) \quad Fb_{meas}(\lambda_2) \quad \cdots \quad Fb_{meas}(\lambda_{211})]^{\mathrm{T}} \\ \boldsymbol{Ff}_{meas} &= [Ff_{meas}(\lambda_1) \quad Ff_{meas}(\lambda_2) \quad \cdots \quad Ff_{meas}(\lambda_{211})]^{\mathrm{T}} \\ F\boldsymbol{b}_{simu} &= [Fb_{simu}(\tau_I,\tau_{II},\delta,\lambda_1) \quad Fb_{simu}(\tau_I,\tau_{II},\delta,\lambda_2) \quad \cdots \quad Fb_{simu}(\tau_I,\tau_{II},\delta,\lambda_{211})]^{\mathrm{T}} \\ F\boldsymbol{f}_{simu} &= [Ff_{simu}(\tau_I,\tau_{II},\delta,\lambda_1) \quad Ff_{simu}(\tau_I,\tau_{II},\delta,\lambda_2) \quad \cdots \quad Ff_{simu}(\tau_I,\tau_{II},\delta,\lambda_{211})]^{\mathrm{T}} \\ \boldsymbol{C}_{nb} &= \mathrm{diag}[\sigma_b(\lambda_1)^2 \quad \sigma_b(\lambda_2)^2 \quad \cdots \quad \sigma_b(\lambda_{211})^2] \\ \boldsymbol{C}_{nf} &= \mathrm{diag}[\sigma_f(\lambda_1)^2 \quad \sigma_f(\lambda_2)^2 \quad \cdots \quad \sigma_f(\lambda_{211})^2] \\ \boldsymbol{x} &= [\tau_I \quad \tau_{II} \quad \delta]^{\mathrm{T}} \\ \boldsymbol{x}_{priori} &= [\tau_I^{priori} \quad \tau_{II}^{priori} \quad \delta^{priori}]^{\mathrm{T}} \\ \boldsymbol{C}_x &= \mathrm{diag}[\sigma(\tau_I)^2 \ \sigma(\tau_{II})^2 \ \sigma(\delta)^2] \end{aligned}$$

where λ_1, λ_2, …, λ_{211} represent the wavelengths of 640 nm, 641 nm, …, 850 nm, respectively. The τ_I, τ_{II}, and δ are the variables during the inversion process. The τ_I^{priori}, τ_{II}^{priori}, and δ^{priori} are the *a priori* guesses of τ_I, τ_{II}, and δ, respectively. The $\sigma(\tau_I)^2$, $\sigma(\tau_{II})^2$, and $\sigma(\delta)^2$ are the variances of the *a priori* guesses of τ_I, τ_{II}, and δ, respectively. The σ_b and σ_f represent the measurement noise of backward and forward fluorescence and uncertainty of model accuracy. The covariance matrices of observation and model uncertainty ($\boldsymbol{C}_{nb}$ and $\boldsymbol{C}_{nf}$) and of the *a priori* variables ($\boldsymbol{C}_x$) determine the respective weights from the measurements and *a priori* knowledge to the cost function. However, their determinations are difficult and somewhat subjective. Detailed discussion on this can be found in [14]. Here, the leaf fluorescence

measurements are considered high quality, especially for the spectral range of 670–800 nm. Therefore, higher weights for these leaf measurements are given than those for *a priori* knowledge.

The first and second terms of the merit function $Ff(\tau_I,\tau_{II},\delta)$ in Equation (9) aim to search for values for the unknown fluorescence parameters (τ_I, τ_{II}, and δ) that best match the simulated backward and forward fluorescence to their correspondingly measured ones, respectively. The third term of the merit function is to inject *a priori* knowledge to the merit function. The *a priori* guesses of τ_I, τ_{II}, and δ (*i.e.*, τ_I^{priori}, τ_{II}^{priori}, and δ^{priori}) were selected as the standard values of τ_I, τ_{II}, and δ given by Pedrós *et al.* [6]. Variances of the *a priori* guesses of τ_I, τ_{II}, and δ (*i.e.*, $\sigma(\tau_I)^2$, $\sigma(\tau_{II})^2$, and $\sigma(\delta)^2$) were estimated by assuming these parameters were uniformly distributed within the variation ranges with the reference given in [6]. The *a priori* knowledge assigned in this study for the unknown parameters is shown in Table 2.

Table 2. *A priori* knowledge for the relative absorption cross section of photosystem I (PSI) and photosystem II (PSII) (δ), the fluorescence lifetimes of PSI and PSII (τ_I and τ_{II}) with the reference given in [6] for the Bayesian inversion of the FluorMODleaf model. The *a priori* knowledge is provided as the *a priori* guesses and the variances of these *a priori* guesses.

Parameter	τ_I	τ_{II}	δ
A priori guess	0.035	0.5	1
Variances of the *a priori* guess	0.0833	0.3333	0.48

The results of the Bayesian inversion procedure contain both the posterior estimates of the unknown parameters of τ_I, τ_{II}, and δ, which are obtained by minimizing the merit function as defined in Equation (9), and the covariance matrix of the posterior estimates, which contains the posterior variances of the inverted values of the unknown parameters. The covariance matrix of the posterior estimates is calculated as:

$$\boldsymbol{C}_{post} = [\boldsymbol{h}_b(\boldsymbol{x}^*)^{\mathrm{T}}\boldsymbol{C}_{nb}^{-1}\boldsymbol{h}_b(\boldsymbol{x}^*) + \boldsymbol{h}_f(\boldsymbol{x}^*)^{\mathrm{T}}\boldsymbol{C}_{nf}^{-1}\boldsymbol{h}_f(\boldsymbol{x}^*) + \boldsymbol{C}_x^{-1}]^{-1} \tag{10}$$

where $\boldsymbol{x}^*$ is a vector that contains the posterior estimates of the unknown parameters of τ_I, τ_{II}, and δ; $\boldsymbol{h}(\boldsymbol{x}^*)$ is the Jacobian matrix for the FluorMODleaf model at the point of $\boldsymbol{x}^*$ and expressed as:

$$\boldsymbol{h}_b(\boldsymbol{x}^*) = \begin{bmatrix} \left.\frac{\partial Fb_{simu}(\lambda_1)}{\partial \tau_I}\right|_{\tau_I=\tau_I^*} & \left.\frac{\partial Fb_{simu}(\lambda_1)}{\partial \tau_{II}}\right|_{\tau_{II}=\tau_{II}^*} & \left.\frac{\partial Fb_{simu}(\lambda_1)}{\partial \delta}\right|_{\delta=\delta^*} \\ \left.\frac{\partial Fb_{simu}(\lambda_2)}{\partial \tau_I}\right|_{\tau_I=\tau_I^*} & \left.\frac{\partial Fb_{simu}(\lambda_2)}{\partial \tau_{II}}\right|_{\tau_{II}=\tau_{II}^*} & \left.\frac{\partial Fb_{simu}(\lambda_2)}{\partial \delta}\right|_{\delta=\delta^*} \\ \vdots & \vdots & \vdots \\ \left.\frac{\partial Fb_{simu}(\lambda_{211})}{\partial \tau_I}\right|_{\tau_I=\tau_I^*} & \left.\frac{\partial Fb_{simu}(\lambda_{211})}{\partial \tau_{II}}\right|_{\tau_{II}=\tau_{II}^*} & \left.\frac{\partial Fb_{simu}(\lambda_{211})}{\partial \delta}\right|_{\delta=\delta^*} \end{bmatrix}$$

$$\boldsymbol{h}_f(\boldsymbol{x}^*) = \begin{bmatrix} \left.\frac{\partial Ff_{simu}(\lambda_1)}{\partial \tau_I}\right|_{\tau_I=\tau_I^*} & \left.\frac{\partial Ff_{simu}(\lambda_1)}{\partial \tau_{II}}\right|_{\tau_{II}=\tau_{II}^*} & \left.\frac{\partial Ff_{simu}(\lambda_1)}{\partial \delta}\right|_{\delta=\delta^*} \\ \left.\frac{\partial Ff_{simu}(\lambda_2)}{\partial \tau_I}\right|_{\tau_I=\tau_I^*} & \left.\frac{\partial Ff_{simu}(\lambda_2)}{\partial \tau_{II}}\right|_{\tau_{II}=\tau_{II}^*} & \left.\frac{\partial Ff_{simu}(\lambda_2)}{\partial \delta}\right|_{\delta=\delta^*} \\ \vdots & \vdots & \vdots \\ \left.\frac{\partial Ff_{simu}(\lambda_{211})}{\partial \tau_I}\right|_{\tau_I=\tau_I^*} & \left.\frac{\partial Ff_{simu}(\lambda_{211})}{\partial \tau_{II}}\right|_{\tau_{II}=\tau_{II}^*} & \left.\frac{\partial Ff_{simu}(\lambda_{211})}{\partial \delta}\right|_{\delta=\delta^*} \end{bmatrix}$$

The posterior standard deviations of the inverted parameters are contained in the main diagonal of $\boldsymbol{C}_{post}$:

$$\boldsymbol{C}_{post} = \begin{bmatrix} \upsilon_{\tau_I}^{\ 2} & \upsilon_{12}^{\ 2} & \upsilon_{13}^{\ 2} \\ \upsilon_{21}^{\ 2} & \upsilon_{\tau_{II}}^{\ 2} & \upsilon_{23}^{\ 2} \\ \upsilon_{31}^{\ 2} & \upsilon_{32}^{\ 2} & \upsilon_{\delta}^{\ 2} \end{bmatrix} \quad (11)$$

where $v_{\tau I}$, $v_{\tau II}$, and v_{δ} are the posterior standard deviations of τ_I^*, τ_{II}^*, and δ, respectively; and the other elements in $\boldsymbol{C}_{post}$ are the covariance values between each two inverted parameters.

The flow diagram of the inversion procedure is illustrated in Figure 3.

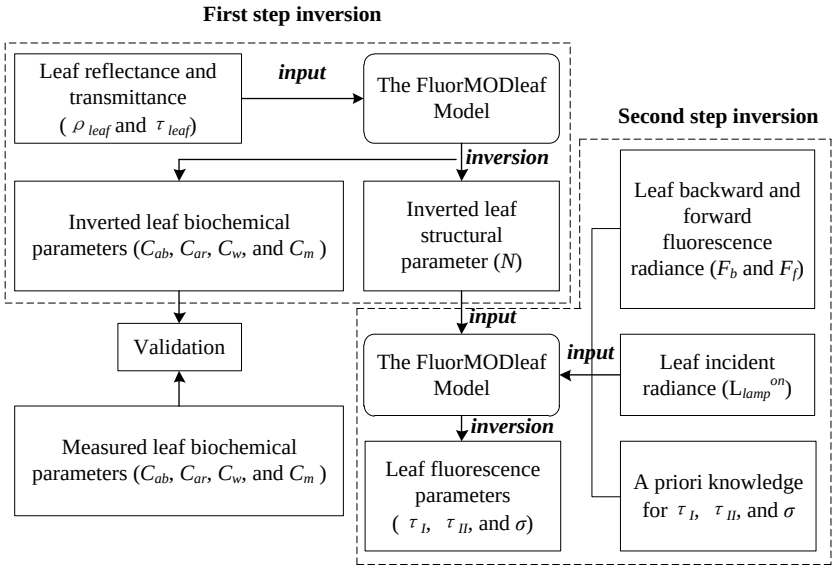

Figure 3. Flow diagram of the retrieval of the fluorescence parameters of plant leaves.

3. Results and Discussion

3.1. Distributions of the Fluorescence Spectra

In Figure 4a, examples of the measured leaf radiance spectra of the sample with and without the filter are shown for the measurement of backward fluorescence; Figure 4b illustrates measurement of forward fluorescence. Corresponding measured leaf fluorescence radiance is also shown in the inset using a finer scale.

In Figure 5, the curves show the mean fluorescence spectra measured in the experiments for crop leaves, and the corresponding shaded areas represent standard deviations of the measured spectra. For the backward fluorescence spectra (Figure 5a,c), two peaks can be observed, with the left one being located approximately at 690 nm and the right one at 740 nm; the right peak higher than the left peak. For the forward fluorescence spectra (Figure 5b,d), the left peak is weak, and almost unnoticeable for wheat leaves (Figure 5b). Highest contrasts between the left and right peaks for both backward and forward fluorescence are observed for soybean leaves (Figure 5c,d). Cotton (Figure 5a,b) and peanut (Figure 5c,d) leaves show relatively lower magnitude of fluorescence, especially for the former. For the peanut leaves (Figure 5c,d), higher variance for both backward and forward fluorescence spectra can be observed. This higher variance was probably caused by the inclusion of the spectra of senescent leaves,

whose left peaks for both backward and forward fluorescence are higher than the right peaks (not shown herein).

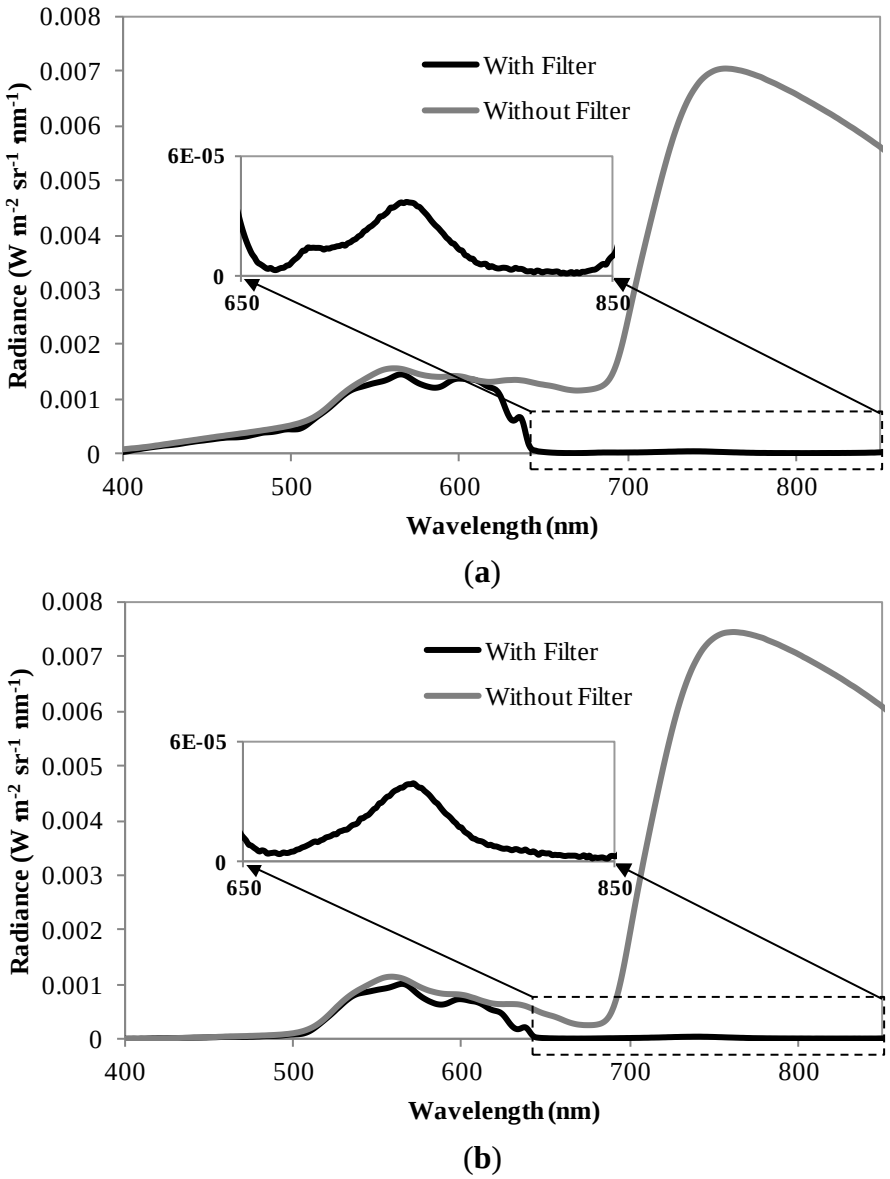

Figure 4. Examples of the radiance spectra of the leaf sample with and without the filter when measuring (**a**) backward fluorescence and (**b**) forward fluorescence. Insets: distributions of measured leaf backward and forward fluorescence radiance with the same unit but in finer scale.

Generally, shapes of the fluorescence spectra and positions of left peak (occurs in the range of 686–691 nm) and right peak (in the range of 739–743 nm) measured in this study are consistent with the spectra measured by a specifically designed equipment (FluoWat) to measure leaf fluorescence reported in other studies [24–26]. However, intensity of the lamp with the filter used in this study is much weaker than that of FluoWat. Thus, values for fluorescence radiance measured here are lower and not directly comparable with those by FluoWat. It can be observed that fluorescence radiance is higher for backward measurements compared with forward measurements for all four crop leaves because absorption and scattering effect are stronger for the forward measurements [27].

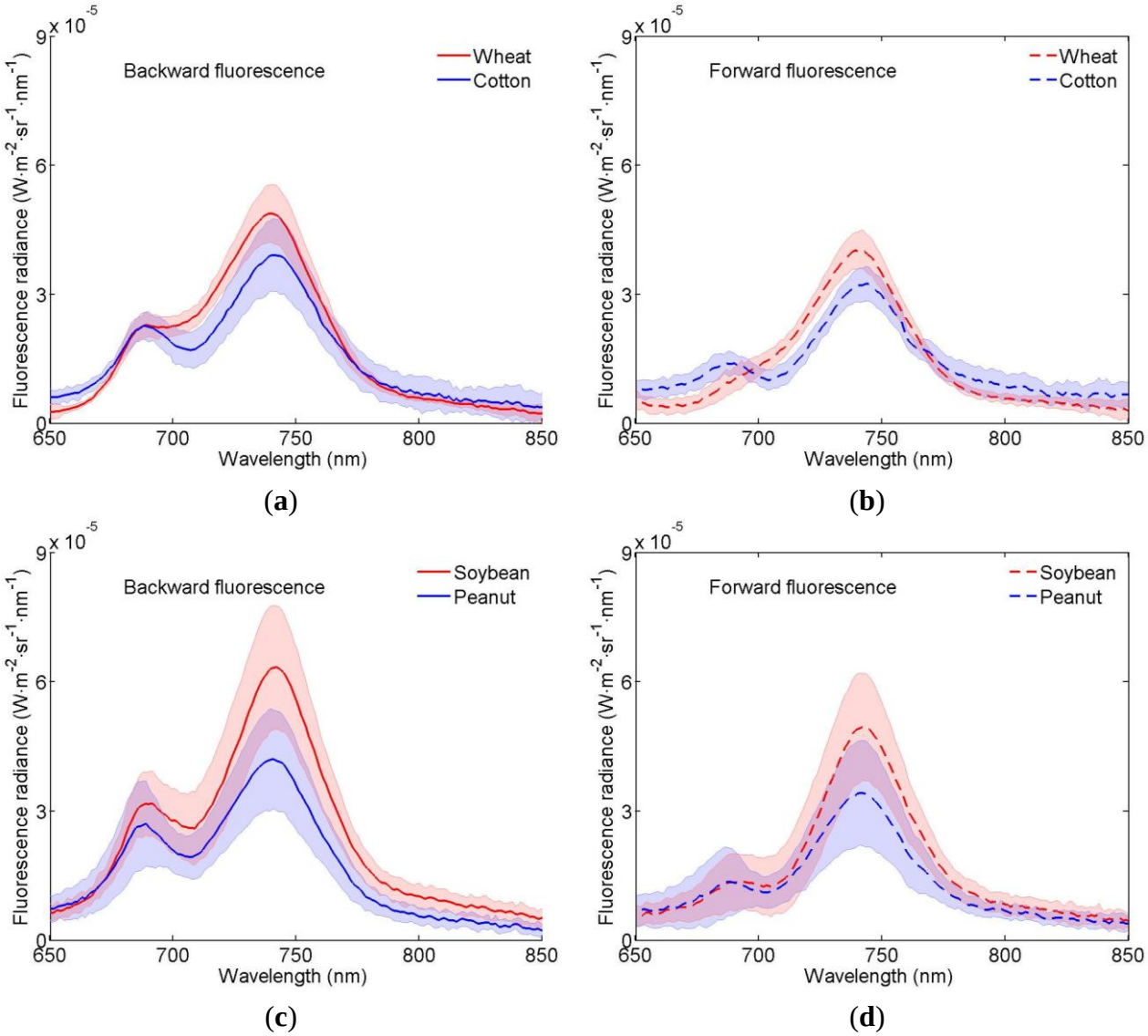

Figure 5. The mean fluorescence spectra measured in the experiments. (**a**) The backward fluorescence spectra for wheat and cotton leaves; (**b**) The forward fluorescence spectra for wheat and cotton leaves; (**c**) The backward fluorescence spectra for soybean and peanut leaves; (**d**) The forward fluorescence spectra for soybean and peanut leaves. The shaded portions represent standard deviation of the measured spectra.

It can also be seen that the fluorescence radiance at right peak is generally higher than the one at left peak. This phenomenon is probably caused by the fact that most leaves chosen in the experiment are green and healthy ones, whose fluorescence emission around left peak subjects to strong re-absorption due to the overlap with red region of chlorophyll absorption. This is especially evident for the forward fluorescence spectra with relatively weaker left peaks, since emitted fluorescence travels from the adaxial to the abaxial leaf side and experiences stronger re-absorption. However for the senescent peanut leaves with low chlorophyll contents, as noted above, the left peaks are higher than the right peaks of both backward and forward fluorescence spectra.

The differences of peak distributions may also be caused by actual engagement of two photosystems. The left peak originates mainly from PS II, while the right peak originates from both PS I and PS II.

Since factors from physiological drivers to environmental drivers can trigger dynamic regulation of the two photosystems [8], magnitudes of the two peaks will be changing accordingly. This reason may explain why the distributions of backward and forward fluorescence between the peaks for wheat leaves are slightly different from those by other three types of crop leaves.

Removal of light with the cut-off filter of 640 nm is biasing the performance of photosynthetic apparatus towards the PS II center, which may additionally affect the peak distributions. Therefore, the noticeable differences in magnitude and subtle distributions of fluorescence for different crops may result from differences in leaf structure of species, pigment contents, and crop physiological conditions.

3.2. Results of Sensitivity Analysis for the FluorMODleaf Model

Results of sensitivity analysis for the FluorMODleaf model are illustrated in Figure 6. Figure 6a shows the first order sensitivity indices of the input parameters of the FluorMODleaf model to the backward fluorescence. The total sensitivity indices of the input parameters are similar to the first order sensitivity indices, and, therefore, are not shown here. It shows that τ_I, τ_{II}, and C_{ab} are the most sensitive parameters among all eight input parameters. The τ_I is more sensitive in the near-infrared region where the PSI contributes the major fluorescence emission, while the τ_{II} is more sensitive in the red region where the PSII is the main photosystem that emits fluorescence. The C_{ab} is a sensitive parameter within the spectral range of 640–850 nm, because it not only has an absorption effect for the emitted ChlF, but it also determines the excitation efficiency of leaves. The C_{ar} is also a relatively sensitive parameter because it partially transfers the absorbed energy to chlorophylls for ChlF emission [6].

For the first order sensitivity indices of the forward fluorescence (Figure 6b), τ_I, τ_{II}, and C_{ab} are still the most influential parameters. It can also be seen that the model becomes relatively sensitive to leaf structural parameter N in the red region compared with its sensitivity of the backward fluorescence. It is because the absorption effect of the leaf biochemical contents (mainly the C_{ab} and C_{ar}) can be indirectly affected by the leaf thickness through the photon's path length, and this effect is more obvious for the forward fluorescence than for the backward fluorescence.

It was also found that the model is relatively insensitive to parameters C_w and C_m with sensitivity indices lower than 0.05 in the wavelength region of 640–850 nm for both the forward and backward fluorescence. This is because the absorption effects of C_w and C_m are relatively insignificant within the ChlF emission region of 640–850 nm.

From the results of sensitivity analysis for FluoMODleaf model, it can be observed that all three fluorescence parameters are relatively influential, although the extents are different for different spectral bands. Thus, it is feasible to invert these parameters from the leaf fluorescence measurements. Three other parameters, C_{ab}, C_{ar}, and N are also sensitive to the leaf fluorescence. However, as inversion studies by using leaf reflectance and transmittance show [9,21], these parameters and other two insensitive parameters, C_w and C_m, for FluorMODleaf, can be successfully inverted by the PROSPECT model. Thus, two stages of inversion were employed: in the first stage, five parameters, N, C_{ab}, C_{ar}, C_w and C_m, were inverted by leaf reflectance and transmittance, and they were fixed at these inverted values; in the second stage, only three fluorescence parameters are changed to optimize the cost function.

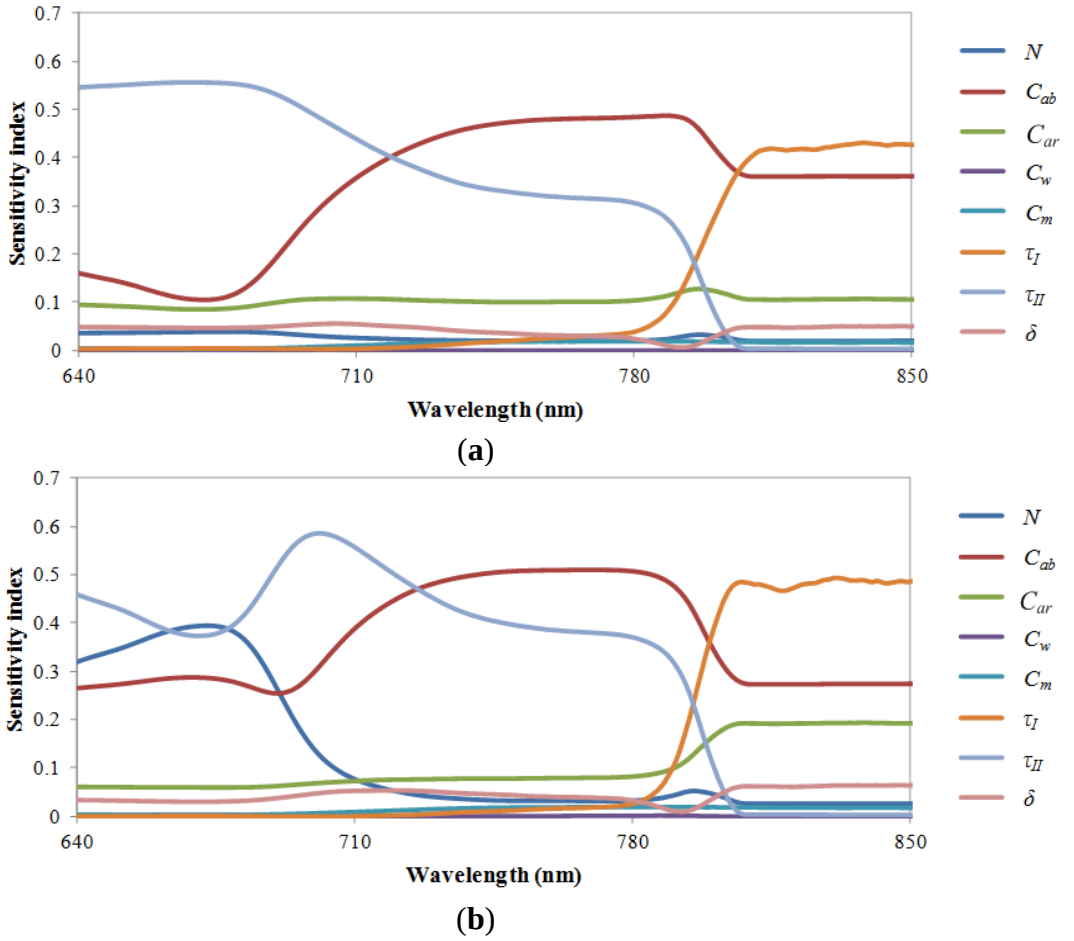

Figure 6. The sensitivity analysis results of the FluorMODleaf model. (**a**) The first order sensitivity indices of the input parameters to the backward fluorescence; (**b**) The first order sensitivity indices of the input parameters to the forward fluorescence.

3.3. Retrieval Results of the Leaf Biochemical Contents

Figure 7 shows the results of the first step inversion for chlorophyll content (C_{ab}), carotenoid content (C_{ar}), water content (C_w), and dry matter content (C_m) for four crops' leaves. The dashed 1:1 line and the equation of regression line are also presented in the figures. It can be observed that retrieved values agree well with their corresponding measured values for C_{ab} (Figure 7a), C_{ar} (Figure 7b) and C_m (Figure 7d). For C_w (Figure 7c), measured values are generally lower than the inverted ones, which is probably caused by the water loss during the later weighting process in the laboratory before oven-drying. It can be found that biochemical contents of peanut leaves cover relatively larger ranges, notably for a low value of C_{ab} around 15 μg/cm^2, which corresponds to the senescent leaves. The coefficient of determination (R^2) and root mean square error (RMSE) between the retrieved and measured values are 0.90 and 3.38 μg/cm^2, 0.83 and 0.93 μg/cm^2, 0.60 and 0.00379 g/cm^2, and 0.61 and 0.00326 g/cm^2, for C_{ab}, C_{ar}, C_w, and C_m, respectively. This generally good agreement between retrieved and measured leaf biochemical contents, especially for the two sensitive parameters for fluorescence, C_{ab} and C_{ar}, assists the second step inversion for the fluorescence parameters.

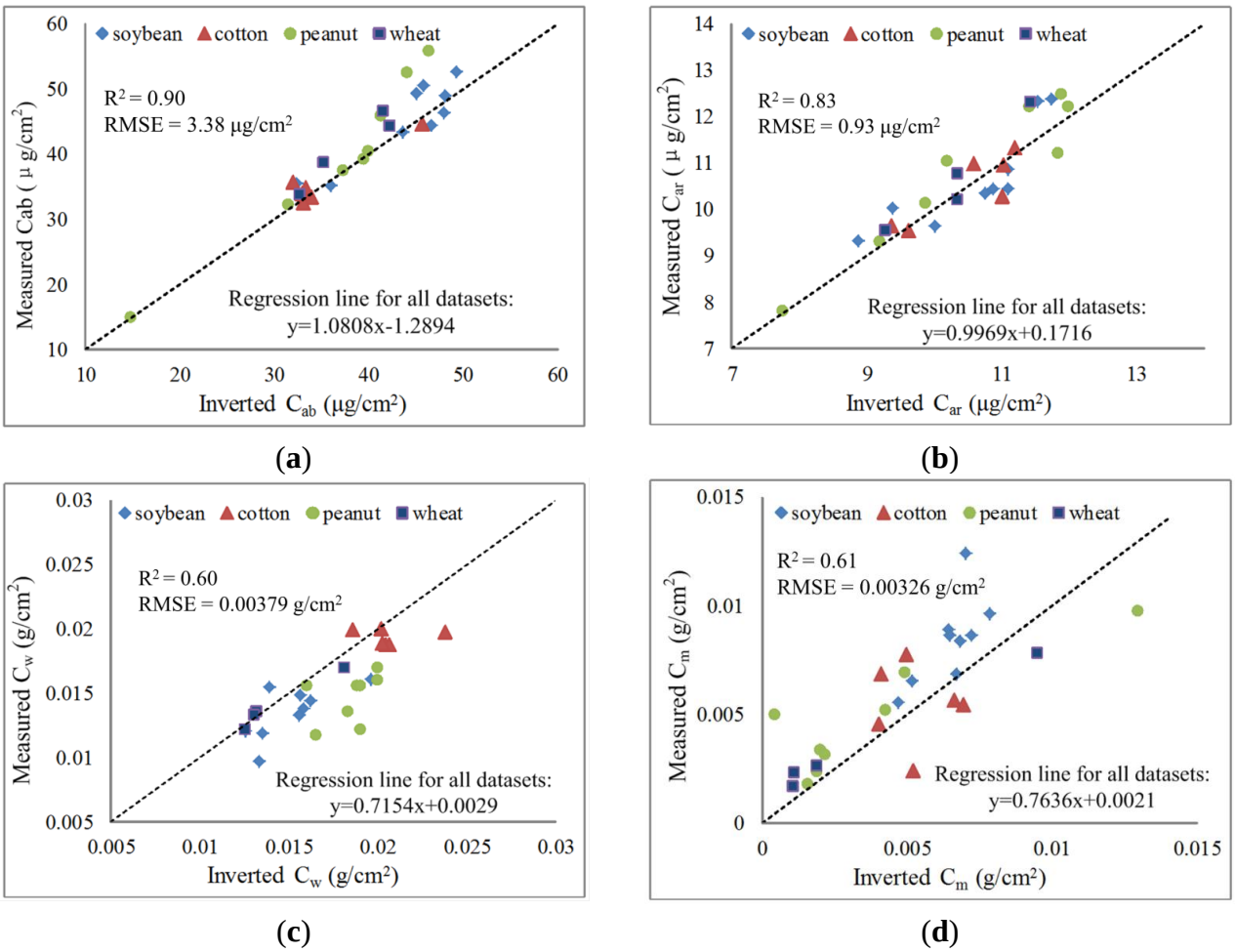

Figure 7. Scatter diagram of inverted and measured values of the chlorophyll content (**a**); carotenoid content (**b**); water content (**c**); and dry matter content (**d**) for four crop leaves. The coefficient of determination (R^2) and root mean square error (RMSE) between the retrieved and measured values are also provided.

3.4. Inversion Results of the Fluorescence Parameters

The fluorescence parameters were retrieved from the leaf spectral measurements by the Bayesian inversion approach. Figure 8 shows the retrieved fluorescence lifetimes of PSI and PSII (τ_I and τ_{II}), the relative absorption cross section of PSI and PSII (δ), and their standard deviations by inverting the FluorMODleaf model for soybean, cotton, peanut and wheat leaves. It can be observed that τ_I is more stable for all four crop types, predominantly in the range of 0.05–0.15 ns. This relatively weak variation is consistent with the assumption that PSI fluorescence does not change with photochemistry, though may change with species [6]. However, for τ_{II}, larger variations within and between species are observed. τ_{II} for soybean is much larger than the other three crops. By comparing the distributions of fluorescence spectra of four crops (Figure 5), we can see that values in the red parts (around the left peak) of the leaf fluorescence spectra for soybean are more distinct and higher than those for other three crops. Since fluorescence emission in this spectral part mainly originates from PSII, higher values of τ_{II}, corresponding to higher contribution from PSII, are obtained. In the FluorMODleaf model, the relative absorption cross section ratio δ affects the fractions of contributions by PSI and PSII to the total

fluorescence, with lower value corresponding to larger contributions from PSI, and higher one to larger contributions from PSII. For our measurements, most leaves show a higher right peak than the left peak, except for some leaves with low chlorophyll contents. Thus, for soybean with the more distinct contrast of fluorescence spectra and wheat with a bit less extent, generally low δ values were obtained. For cotton and peanut leaves with relatively weak contrast between the left and right peaks, δ values are generally higher. For the senescent peanut leaves, inverted δ reaches 1.71. The inverted values of δ here are generally lower than the values suggested by Pedrós *et al.* [6]. Besides, the aforementioned features of measured fluorescence data, this difference may also be caused by the different experimental setup and light source used in our experiment. Another output of the Bayesian inversion with the inverted parameters is their corresponding posterior standard deviations. These posterior standard deviations are always lower than the standard deviations of the *a priori* guess, which shows the reduction of uncertainty of model parameters during the inversion.

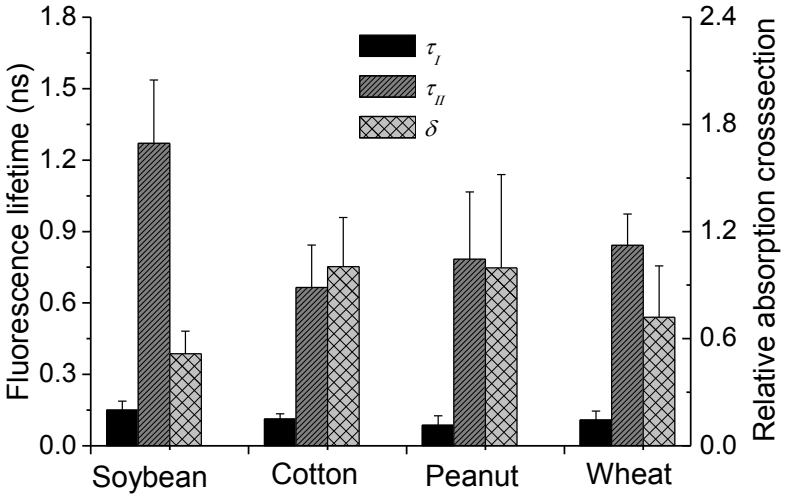

Figure 8. The fluorescence lifetimes of PSI and PSII (τ_I and τ_{II}), the relative absorption cross section of PSI and PSII (δ), and the standard deviations by inverting the FluorMODleaf model for four crops' leaves.

Although different leaves of the crops at different times in a day were sampled in the measurement, the results show that the fluorescence parameters are species-dependent and sensitive to biochemical contents and environmental factors. Because of the complexity of the relationship between fluorescence emission and the plant physiology, it is difficult at this stage to quantitatively interpret physiological meaning of these inverted fluorescence parameters. Further studies with simultaneous measurement of photosynthetic functions and fluorescence emission spectra are needed to better understand these parameters.

These fluorescence parameters are difficult to measure directly, and consequently it is difficult to evaluate the inversion results through measurements. As an alternative, the fluorescence spectra reconstructed from the inverted fluorescence parameters and measured in the experiment, both with a step of 1 nm, were then compared. The comparison results are shown in Figure 9a,b for leaf backward and forward fluorescence, respectively. R^2 and RMSE are 0.96 and 3.14 × 10^{-6} W m^{-2} sr^{-1} nm^{-1}, respectively, for backward fluorescence, and 0.92 and 3.84 × 10^{-6} W m^{-2} sr^{-1} nm^{-1} for forward fluorescence, which indicates a high accuracy of the inversion results. The reconstructed and measured

fluorescence radiances at two peaks (690 and 740 nm) are also presented in the insets, which do not show systematic deviations between them.

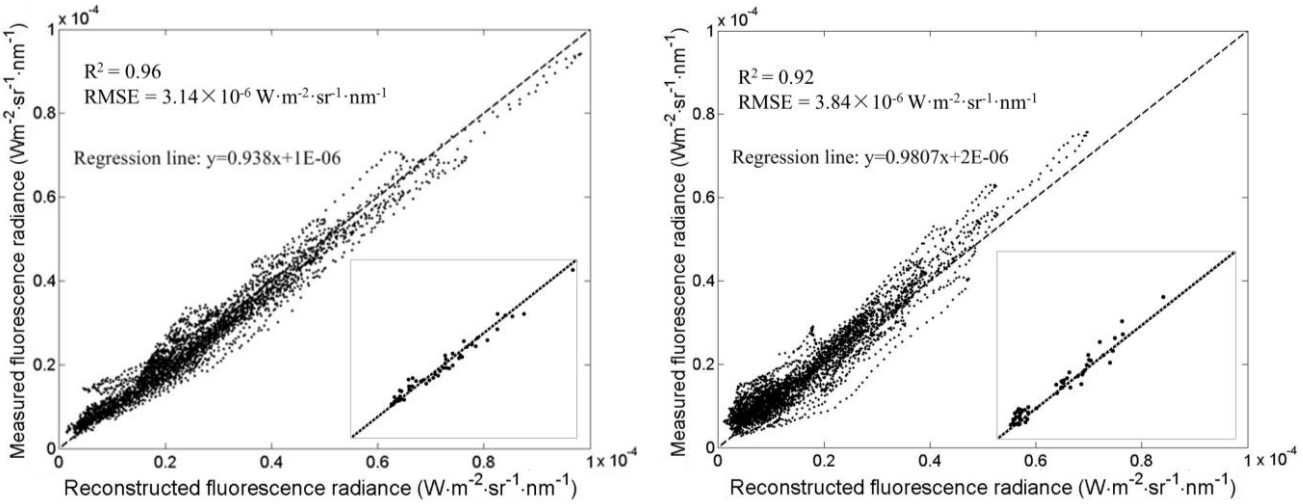

Figure 9. Comparison between the leaf fluorescence radiance spectra reconstructed from the inverted fluorescence parameters and the leaf fluorescence radiance spectra measured in the experiment for (**a**) backward and (**b**) forward fluorescence radiance. Insets: Comparison between reconstructed and measured fluorescence radiances at 690 and 740 nm with the same unit.

3.5. Potential and Limitations of Applying Model Inversion for the Retrieval of Leaf Fluorescence Parameters

The ChlF signal can provide critical information about the growth status of plants, and therefore it has been used as an effective tool to monitor plant stress induced by air pollution [25,26], water deficit [28,29], herbicide treatment [2], and salt and drought [30]. Quantitative estimation of the fluorescence parameters for crop leaves would be of high importance in assessing the photosynthetic rates of green plants and monitoring the stress conditions of crops. In this study, the leaf-level FluorMODleaf model was inverted using the leaf fluorescence spectra measured in the experiments. Results indicate that, even though the ChlF signal is relatively weak, the fluorescence parameters can be reliably inverted by introducing two stages inversion and adopting the Bayesian-based inversion strategy. However, this conclusion comes from an indirect way: inverted fluorescence parameters are generally in the reasonable ranges, there are no high and systematic deviations between measured fluorescence and re-constructed fluorescence, and the posterior standard deviations are always lower than the standard deviations of the *a priori* guess. More experiments can be designed and conducted to further evaluate the inversion strategy and better investigate the potential of the inverted fluorescence parameters in crop stress detections and growth status monitoring. Moreover, for practical applications of remote sensing technique, canopy-level ChlF model can be simulated in order to interpret the canopy fluorescence signal from the airborne and space-borne observations. With the fast development of the vegetative canopy models based on the radiative transfer theory [8,31–33] and the computer simulation

methods [34], coupling the leaf-level ChlF model (e.g., FluorMODleaf) with a canopy-level ChlF models can become a promising tool for the growth status monitoring of crops in precision agriculture.

Indeed, the incident radiance between 640–700 nm can also excite fluorescence. However, the processes to emit fluorescence and reflect (and transmit) the incident radiation occur simultaneously, thus making the separation of the fluorescence from the total radiation very challenging. In order to ensure that the entire leaf fluorescence spectra of 640–850 nm could be obtained, the short-pass filter with the cut-off wavelength of 640 nm was used in the experiment, which blocked the lamp radiance between 640–700 nm and consequently the reflected and transmitted radiance from the lamp. This experimental setup provides an effective and efficient method to non-destructively obtain the leaf ChlF spectra. The intensity of the lamp used in this study is weak enough to avoid the influence to the photosynthetic process and induction of variable fluorescence. However, the removal of excitation radiation from 640–700 may induce potential bias in the measured ChlF spectra, which needs further investigation. In the future studies, filters with different cut-off wavelengths can be used to measure leaf ChlF spectra to compare the inversion results.

4. Conclusions

Leaf ChlF is closely related to the photosynthetic conditions of green plants. In this study, a sensitivity analysis of the FluorMODleaf model was performed using the EFAST method. Based on the sensitivity analysis results, the FluorMODleaf model was inverted using the experimental datasets. Bayesian theory was introduced to the inversion process aiming to achieve a stable inversion results. Results showed that R^2 and RMSE between the fluorescence simulated from the inverted fluorescence parameters and measured in the experiment were 0.96 and 3.14×10^{-6} W m^{-2} sr^{-1} nm^{-1}, respectively, for backward fluorescence, and 0.92 and 3.84×10^{-6} W m^{-2} sr^{-1} nm^{-1} for forward fluorescence. Based on results, it can be concluded that the Bayesian inversion approach can be used to retrieve the fluorescence parameters of plant leaves by inverting the FluorMODleaf model. The retrieved fluorescence parameters have the potential for agricultural applications.

Acknowledgments

This work is supported by the Chinese Natural Science Foundation under Project 41371325. Thanks go to Xu Dai and Peng Zhang for their assistance during the experiment. The authors are grateful to Yves Goulas, Roberto Pedrós, and Fabrice Daumard, for providing the codes of the FluorMODleaf model and helpful comments. Feng Zhao would like to express his appreciation for the assistance given by E.L. Butt-Castro (Tina) and J. de Koning (Anke) during his visit at Faculty of Geo-Information Science and Earth Observation (ITC), University of Twente. The authors thank Steven J. Thomson for polishing the manuscript. The authors also thank the reviewers for thoroughly reading the paper and providing useful suggestions.

Author Contributions

Feng Zhao conceived the research, proposed the research method, conducted the data analysis, prepared the manuscript and made the revision. Yiqing Guo contributed to the data analysis and the

manuscript preparation. Yanbo Huang contributed to the research method and the manuscript revision. Wout Verhoef and Christiaan van der Tol provided suggestions for the research method and manuscript revision. Bo Dai contributed to the data analysis. Liangyun Liu contributed to the design of field experiment, and provided suggestions for the manuscript revision. Huijie Zhao provided suggestions for the research and manuscript revision. Guang Liu contributed to the design of field experiment and the manuscript revision.

Conflicts of Interest

The authors declare no conflict of interest.

References

1. Meroni, M.; Rossini, M.; Guanter, L.; Alonso, L.; Rascher, U.; Colombo, U.; Moreno, J. Remote sensing of solar-induced chlorophyll fluorescence: Review of methods and applications. *Remote Sens. Environ.* **2009**, *113*, 2037–2051.
2. Huang, Y.; Thomson, S.J.; Molin, W.T.; Reddy, K.N.; Yao, H. Early detection of soybean plant injury from glyphosate by measuring chlorophyll reflectance and fluorescence. *J. Agric. Sci.* **2012**, *4*, 117–124.
3. Zhao, F.; Guo, Y.; Huang, Y.; Reddy, K.N.; Zhao, Y.; Molin, W.T. Detection of the onset of glyphosate-induced soybean plant injury through chlorophyll fluorescence signal extraction and measurement. *J. Appl. Remote Sens.* **2015**, *9*, doi:10.1117/1.JRS.9.097098.
4. Guanter, L.; Zhang, Y.; Jung, M.; Joiner, J.; Voigta, M.; Berry, J.A.; Frankenberg, C.; Huete, A.R.; Zarco-Tejada, P.; Lee, J.-E.; *et al.* Global and time-resolved monitoring of crop photosynthesis with chlorophyll fluorescence. *Proc. Natl. Acad. Sci. USA* **2014**, *111*, E1327–E1333.
5. Sušila, P.; Nauš, J. A Monte Carlo study of the chlorophyll fluorescence emission and its effect on the leaf spectral reflectance and transmittance under various conditions. *Photochem. Photobiol. Sci.* **2007**, *6*, 894–902.
6. Pedrós, R.; Goulas, Y.; Jacquemoud, S.; Louis, J.; Moya, I. FluorMODleaf: A new leaf fluorescence emission model based on the PROSPECT model. *Remote Sens. Environ.* **2010**, *114*, 155–167.
7. Verhoef, W. Modeling vegetation fluorescence observations. In Proceedings of the EARSel 7th SIG-Imaging Spectroscopy Workshop, Edinburgh, UK, 11–13 April 2011.
8. Miller, J.R.; Berger, M.; Goulas, Y.; Jacquemoud, S.; Louis, J.; Mohammed, G.; Moise, N.; Moreno, J.; Moya, I.; Pedrós, R.; *et al*. *Development of A Vegetation Fluorescence Canopy Model*; ESTEC Contract No. 1635/02/NL/FF; ESA Scientific and Technical Publications Branch, ESTEC: Paris, French, 2015.
9. Feret, J.-B.; François, C.; Asner, G.P.; Gitelson, A.A.; Martin, R.E.; Bidel, L.P.R.; Ustin, S.L.; Le Maire, G.; Jacquemoud, S. PROSPECT-4 and 5: Advances in the leaf optical properties model separating photosynthetic pigments. *Remote Sens. Environ.* **2008**, *112*, 3030–3043.
10. Jacquemoud, S.; Baret, F. PROSPECT: A model of leaf optical properties spectra. *Remote Sens. Environ.* **1990**, *34*, 75–91.
11. Li, X.; Gao, F.; Wang, J.; Strahler, A. A priori knowledge accumulation and its application to linear BRDF model inversion. *J. Geophys. Res. D: Atmos.* **2001**, *106*, 11925–11935.

12. Laurent, V.C.E.; Schaepman, M.E.; Verhoef, W.; Weyermann, J.; Chávez, R.O. Bayesian object-based estimation of LAI and chlorophyll from a simulated Sentinel-2 top-of-atmosphere radiance image. *Remote Sens. Environ.* **2014**, *140*, 318–329.
13. Wang, Y.; Li, X.; Nashed, Z.; Zhao, F.; Yang, H.; Guan, Y.; Zhang, H. Regularized kernel-based BRDF model inversion method for ill-posed land surface parameter retrieval. *Remote Sens. Environ.* **2007**, *111*, 36–50.
14. Laurent, V.C.E.; Verhoef, W.; Damm, A.; Schaepman, M.E.; Clevers, J.G.P.W. A Bayesian object-based approach for estimating vegetation biophysical and biochemical variables from at-sensor APEX data. *Remote Sens. Environ.* **2013**, *139*, 6–17.
15. Zarco-Tejada, P.J.; Miller, J.R.; Mohammed, G.H.; Noland, T.L. Chlorophyll fluorescence effects on vegetation apparent reflectance: I. Leaf-Level measurements and model simulation. *Remote Sens. Environ.* **2000**, *74*, 582–595.
16. Zhang, Y. Studies on Passive Sensing of Plant Chlorophyll Florescence and Application of Stress Detection. Ph.D. Thesis, Zhejiang University, Hangzhou, China, May 2006; pp. 24–27.
17. LI-COR Inc. *LI-COR LI-1800-12 Integrating Sphere Instruction Manual*; LI-COR Inc.: Lincoln, NE, USA, 1983.
18. Lichtenthaler, H.K.; Buschmann, C. Extraction of photosynthetic tissues: Chlorophylls and carotenoids. In *Current Protocols in Food Analytical Chemistry*; Wrolstad, R.E., Acree, T.E., Decker, E.A., Penner, M.H., Reid, D.S., Schwarts, S.J., Eds.; John Wiley and Sons: New York, NY, USA, 2001; p. F4.2.1-6.
19. Saltelli, A.; Ratto, M.; Andres, T.; Campolongo, F.; Cariboni, J.; Gatelli, D.; Saisana, M.; Tarantola, S. *Global Sensitivity Analysis, the Primer*; John Wiley & Sons Ltd.: West Sussex, UK, 2008.
20. Saltelli, A.; Tarantola, S.; Chan, K. A quantitative, model independent method for global sensitivity analysis of model output. *Technometrics* **1999**, *41*, 39–56.
21. Zhao, F.; Guo, Y.; Huang, Y.; Reddy, K.N.; Lee, M.A.; Fletcher, R.S.; Thomson, S.J. Early detection of crop injury from herbicide glyphosate by leaf biochemical parameter inversion. *Int. J. Appl. Earth Observ. Geoinf.* **2014**, *31*, 78–85.
22. Zhao, F.; Huang, Y.; Guo, Y.; Reddy, K.N.; Lee, M.A.; Fletcher, R.S.; Thomson, S.J.; Zhao, H. Early detection of crop injury from glyphosate on soybean and cotton using plant leaf hyperspectral data. *Remote Sens.* **2014**, *6*, 1538–1563.
23. Liu, Q. Study on Component Temperature Inversion Algorithm and the Scale Structure for Remote Sensing Pixel. Ph.D. Thesis, Institute of Remote Sensing Applications, Chinese Academy of Sciences, Beijing, China, May 2002.
24. Van Wittenberghe, S.; Alonso, L.; Verrelst, J.; Moreno, J.; Samson, R. Bidirectional sun-induced chlorophyll fluorescence emission is influenced by leaf structure and light scattering properties—A bottom-up approach. *Remote Sens. Environ.* **2015**, *158*, 169–179.
25. Van Wittenberghe, S.; Alonso, L.; Verrelst, J.; Verrelst, I.; Delegido, J.; Veroustraete, F.; Veroustraete, R.; Moreno, J.; Samson, R. Upward and downward solar-induced chlorophyll fluorescence yield indices of four tree species as indicators of traffic pollution in Valencia. *Environ. Poll.* **2013**, *173*, 29–37.

26. Van Wittenberghe, S.; Alonso, L.; Verrelst, J.; Hermans, I.; Valcke, R.; Veroustraete, F.; Moreno, J.; Samson, R. A field study on solar-induced chlorophyll fluorescence and pigment parameters along a vertical canopy gradient of four tree species in an urban environment. *Sci. Total Environ.* **2014**, *466–467*, 185–194.
27. Louis, J.; Cerovic, Z.G.; Moya, I. Quantitative study of fluorescence excitation and emission spectra of bean leaves. *J. Photochem. Photobiol. B* **2006**, *85*, 65–71.
28. Zarco-Tejada, P.J.; Berni, J.A.J.; Suárez, L.; Sepulcre-Cantó, G.; Morales, F.; Miller, J.R. Imaging chlorophyll fluorescence with an airborne narrow-band multispectral camera for vegetation stress detection. *Remote Sens. Environ.* **2009**, *113*, 1262–1275.
29. Zarco-Tejada, P.J.; González-Dugo, V.; Berni, J.A.J. Fluorescence, temperature and narrow-band indices acquired from a UAV platform for water stress detection using a micro-hyperspectral imager and a thermal camera. *Remote Sens. Environ.* **2012**, *117*, 322–337.
30. Naumann, J.C.; Young, D.R.; Anderson, J.E. Linking leaf chlorophyll fluorescence properties to physiological responses for detection of salt and drought stress in coastal plant species. *Physiol. Plant.* **2007**, *131*, 422–433.
31. Verhoef, W. Light scattering by leaves with application to canopy reflectance modelling: The SAIL model. *Remote Sens. Environ.* **1984**, *16*, 125–178.
32. Van der Tol, C.; Verhoef, W.; Timmermans, J.; Verhoef, A.; Su, X. An integrated model of soil-canopy spectral radiances, photosynthesis, fluorescence, temperature and energy balance. *Biogeosciences* **2009**, *6*, 3109–3129.
33. Zhao, F.; Gu, X.; Verhoef, W.; Wang, Q.; Yu, T.; Liu, Q.; Huang, H.; Qin, W.; Chen, L.; Zhao, H. A spectral directional reflectance model of row crops. *Remote Sens. Environ.* **2010**, *114*, 265–285.
34. Zhao, F.; Li, Y.; Dai, X.; Verhoef, W.; Guo, Y.; Shang, H.; Gu, X.; Huang, Y.; Yu, T.; Huang, J. Simulated impact of sensor field of view and distance on field measurements of bidirectional reflectance factors for row crops. *Remote Sens. Environ.* **2015**, *156*, 129–142.